



ACADEMIC
PRESS

Available online at www.sciencedirect.com

SCIENCE @ DIRECT®

Icarus 162 (2003) 183–189

ICARUS

www.elsevier.com/locate/icarus

Gas trapping in water ice at very low deposition rates and implications for comets

G. Notesco,^a A. Bar-Nun,^{a,*} and T. Owen^b

^a *Department of Geophysics and Planetary Sciences, Tel-Aviv University, Tel-Aviv 69978, Israel*

^b *Institute for Astronomy, University of Hawaii, Honolulu, HI 96822, USA*

Received 20 May 2002; revised 14 October 2002

Abstract

The effect of water ice formation temperature and rate of ice deposition on a cold plate on the amount of trapped argon (equivalent to CO), and the ratios of Ar/Kr/Xe trapped in the water ice were studied at 50, 27 and 22 K and at ice formation rates ranging over four orders of magnitude, from 10^{-1} to 10^{-5} $\mu\text{m min}^{-1}$. Contrary to our previous conclusions that cometary ices were formed at 50–60 K, we now conclude that these ices were formed at about 25 K. At 25 K the enrichment ratios for Ar, Kr, and Xe remained the same as those at 50 K, reinforcing our suggestion of cometary contribution of these noble gases to the atmospheres of Earth and Mars.

© 2003 Elsevier Science (USA). All rights reserved.

Keywords: Atmospheres, evolution; Comets; Comets, origin; Ices

Introduction

The role of comets in bringing a major fraction of the volatiles to the forming Earth has always seemed important, but has been difficult to establish with certainty (Sill and Wilkening, 1978; Delsemme 1991, 2000; Owen and Bar-Nun, 1995, 2000). One obvious test is a comparison of the isotope ratio D/H in cometary water with the value of 1.6×10^{-4} found in the Earth's oceans. The D/H ratio in the Oort cloud comets Halley, Hale-Bopp, and Hytaketake is only twice the value found in the Earth's oceans, yet the oceanic D/H is nearly 10 times higher than the value of D/H in solar nebula hydrogen (Laufer et al., 1999). Evidently the water ice in Oort cloud comets never fully equilibrated with solar nebula hydrogen. Thus for comets to be a major source of ocean water, one needs to invoke a different type of comet from the three that have been measured so far (Delsemme, 2000) or one needs some other source of water with D/H lower than the value we now find in seawater (perhaps more fully equilibrated) to blend with the cometary water to make the oceans (Owen and Bar-Nun, 2000).

Another test of possible cometary contributions is provided by the relative abundances of Ar, Kr, and Xe in the atmospheres of Earth and Mars. The proportions of these three heavy noble gases in both planetary atmospheres are remarkably similar, and completely different from the abundances found in meteorites or the solar wind. The dominating characteristics of the atmospheric mixture are a depletion of Ar/Kr by a factor of 100 compared to the solar value and an increase in Kr/Xe by a factor 20 compared with gases found in meteorites. We have reproduced these two characteristics in laboratory experiments in which an originally solar mixture of Ar, Kr, and Xe + water-vapor was flowed onto a cold plate at 50–55 K. The gases were trapped in the amorphous ice in ratios different than that in the original mixture, namely fractionated (Owen et al., 1991, 1992; Owen and Bar-Nun, 1993). The ice must be amorphous, with many pores in which the gases reside, attracted to the ice by Van der Waals forces, which differ from gas to gas, until an ice layer forms over the open pores (Owen et al., 1991; Notesco and Bar-Nun, 1997; Notesco et al., 1999a).

From experiments with trapped gases such as CO, CH₄, C₂H₆, Ar, Kr, Xe in water ice and the observed cometary abundance of ~10% of CO, we suggested that the ice

* Corresponding author. Fax: +972-3-640-9282.

E-mail address: aktivab@luna.tau.ac.il (A. Bar-Nun).

particles that agglomerated to form comets like Halley, Hyakutake, and Hale–Bopp were formed at about 50–60 K (Bar-Nun and Kleinfeld, 1989; Notesco et al., 1997, 1999b). However, these gas-laden amorphous ice samples were produced at a rather high flow rate onto the cold plate: $\sim 10\text{-}\mu\text{m}$ -thick ice layers were formed during ~ 10 min. In this case, the pores in which the gases reside were covered rather quickly, trapping Ar, Kr, and Xe in the right proportion at ~ 50 K. However, given the low densities expected in the natural environment, it is more realistic to assume that the formation of ice grains, either in the interstellar cloud or the outer solar nebula, took thousands or millions of years, so we studied the effect of changing the rate of deposition over four orders of magnitude on the amounts of trapped gases and on the fractionation factors for Ar, Kr, and Xe. Obviously one cannot wait millions of years to form an ice grain in the laboratory, but the trend in the experimentally measured gas trapping might indicate what happened when these ice grains were formed at very low rates.

Two sets of experiments were performed: In the first one, the amount of trapped argon in water ice was measured as a function of the deposition rate and the temperature of the cold plate, in order to determine how much Ar can be trapped in the ice. The trapping efficiency of Ar is very similar to that of CO, the main gas trapped in comet nuclei (Bar-Nun et al., 1988). Thus with appropriate care, the results obtained for Ar can be extended to CO.

In the second, the ratios of Ar/Kr/Xe were studied in order to find out whether comets formed at the temperature required to obtain the observed CO/H₂O ratio can also produce the Ar/Kr/Xe ratios in Earth's and Mars' atmosphere as suggested by Owen et al., (1991, 1992) and Owen and Bar-Nun (1993).

Experimental

The experimental setup was described in previous papers (Bar-Nun et al., 1985, 1987). Water-vapor:Ar = 1:1 mixtures were flowed onto a cold plate in a cryogenically pumped chamber at 10^{-8} Torr. Ice layers about $0.1\ \mu\text{m}$ thick (assuming a density of $0.5\ \text{g cm}^{-3}$) were deposited during different time periods of 0.75 to 4440 min. The deposition rate was varied by two needle-valves between the water-vapor + gas mixture bulb and the mixture introduction tube with a diffuser at its end. In order to decrease the water flow, we placed the bulb containing the water-vapor + gas mixture in a cooled ethanol bath, decreasing the water-vapor pressure and, consequently the deposition rate to about $10^{-5}\ \mu\text{m min}^{-1}$. The water-vapor + Ar mixture was prepared as follows: into a 2-L glass bulb, cooled in an ethanol bath, thoroughly degassed water-vapor from another bulb was introduced until some water ice accumulated on the walls. The water-vapor pressure was then measured and an identical pressure of Ar was added. The cold plate's temperature was varied from 50 to 37, 27, and 22 K.

After the deposition was finished, a sequence of warming-up steps was initiated: the plate was warmed at a rate of $10\ \text{K min}^{-1}$ until the Ar frozen on it sublimated completely (at ~ 45 K). During this period, the temperature of the cold finger, which cools the plate, increased from ~ 20 K by only 1–2 K but continued to warm up and release the Ar, which was frozen on it up to ~ 35 K. To clean it further, the temperature of the cold finger was raised until the last traces of frozen Ar on it sublimated. The Ar flux during the cleaning stage of the cold finger was omitted from Fig. 1 and the curves were smoothed between ~ 45 and 120 K. When the Ar flux leveled off, the plate's warming was resumed, at a rate of $1\text{--}2\ \text{K min}^{-1}$, under constant cryopumping, until the ice sublimated completely. The fluxes of the gas and the water-vapor evolving from the ice were monitored by a quadrupole mass spectrometer, and their total amount was obtained by integrating their flux over time. After each experiment, the system was calibrated with the same water-vapor + Ar mixture immersed in the ethanol bath, while the chamber was at room temperature.

In another set of experiments, water-vapor:Ar:Kr:Xe = 100:100:1:2 mixtures were flowed onto the plate, in order to restudy the enrichment ratios of the noble gases when they are trapped in water ice. This Ar:Kr:Xe ratio was chosen because lower amounts of Kr and Xe (like the solar nebula's ratio of the most abundant nonradiogenic heavy noble gases Ar:Kr:Xe = 69000:21:1) could not be detected in the experiments.

Results and discussion

A typical plot of the gas and water emerging from ice upon warming is shown in Fig. 1. Argon is released from the ice in two major temperature ranges: 30–45 K, where the frozen gas evaporates from the ice surface, and 135–155 K, where the amorphous water ice changes into a high-viscosity "liquid" with $\sim 30\%$ of cubic domains (Jenniskens and Blake, 1994, 1996), accompanied by the opening of blocked pores, thus releasing the gas trapped in the water ice (Laufer et al., 1987; Bar-Nun et al., 1988). No gas is retained in the ice beyond this dynamic percolation process because the ice layer is very thin (Notesco et al., 1991).

As seen in Fig. 1, very large amounts of frozen Ar, much more than the amount of water ice, accumulate at 27 and 22 K at high deposition rates. Previously (Laufer et al., 1987), we attributed this high gas/ice ratio to the ejection of ice grains from the ice, propelled by gas jets, both of which were observed by the mass spectrometer. However, this explanation is not valid for very thin ice layers, where no grains or jets were observed. Alternatively, the Ar atoms and H₂O molecules have two different tracks in the chamber: when a stream of water-vapor with Ar is directed at the 27- or 22-K deposition plate, the water molecules freeze to form the highly porous structure of amorphous ice. Argon atoms enter these pores and, if they reside there long

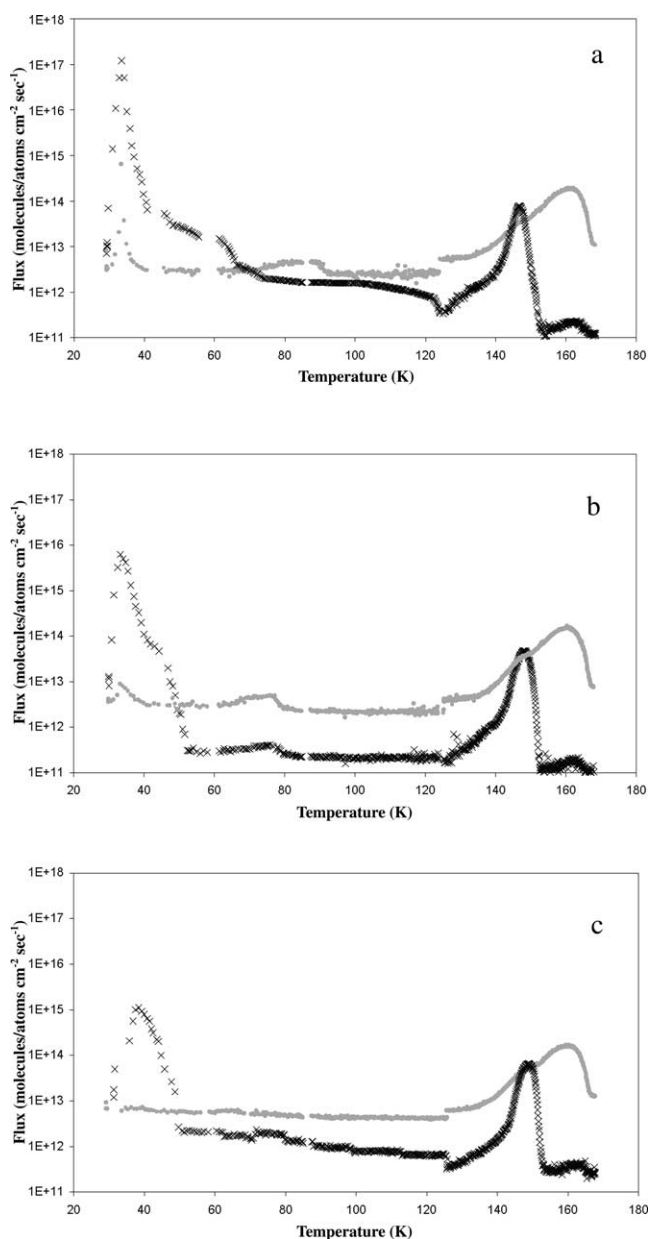


Fig. 1. A plot of the fluxes of evolved Ar (black curve) and water (gray curve) during warming up of the ice. The gas-laden ice was deposited at 27 K from a $\text{H}_2\text{O}:\text{Ar} = 1:1$ mixture, at rates of (a) 10^{-1} , (b) 10^{-3} , and (c) $10^{-4} \mu\text{m min}^{-1}$. Note the drop in the amount of frozen argon (30–45 K) by an order of magnitude for each order of magnitude of decrease in the rate of deposition. This obviously means that at very low rates of deposition the amount of frozen Ar will become negligible. On the other hand, the amount of trapped Ar, which is released between 135 and 155 K, remains constant.

enough, by Van der Waals attraction forces, and another ice layer forms above the pores, the Ar is trapped inside the ice. Water molecules that do not stick to the forming ice layer make one journey in the chamber until they hit the $\sim 90\text{-K}$ radiation shield and freeze there. The Ar atoms on the other hand do not freeze on the radiation shield, nor are they trapped in the $\sim 90\text{-K}$ ice. Consequently, they journey in the chamber until they are pumped by the cryopump. (We

should bear in mind that only 10% of the gas is trapped in the ice while most of it is not trapped.) Therefore, the partial pressure of Ar in the chamber is considerably larger than that of the water molecules. This “background” Ar can be also trapped in the open pores of the ice, but most of it freezes on the ice whose surface area was measured by us to be $86 \text{ m}^2 \text{ g}^{-1}$ at 44 K (Bar-Nun et al., 1987), decreasing at higher temperatures and most likely being larger at 27 or 22 K. The very large amount of frozen Ar that accumulates on the cold finger, which is situated behind the deposition plate, is indicative of this process. The decrease in the amount of frozen Ar with decreasing deposition rates (Fig. 1) is also indicative, since then the lower flux of Ar can be picked up by the cryopump, and even more so when a small flux of Ar is released from the ice sample. The latter was demonstrated in various previous experiments where the rate of warming up of the ice was changed by up to 10-fold and the measured ratio of frozen or trapped Ar to H_2O was found to be constant, showing that the efficiency of the pumping system is large enough.

The amount of Ar trapped in water ice formed at 50 K decreases as the deposition rate decreases (Fig. 2a), and becomes smaller than the critical 10% (the amount of CO in the three studied comets) already at a deposition rate of $10^{-3} \mu\text{m min}^{-1}$. This is because at a lower deposition rate the open ice pores are covered more slowly by overlying water ice from further deposition and the gas atoms can leave the open pores before they are covered. We have already shown (Notesco et al., 1999a) that $^{40}\text{Ar}/^{36}\text{Ar}$, $^{84,86}\text{Kr}/^{82}\text{Kr}$ isotope enrichments, when trapped in water ice, depend on the square root of their masses due to their thermal energy ($\frac{1}{2}mv^2$), which is obviously higher at 50 K than at 27 or 22 K. An enrichment in the Xe isotopes could not be detected because of their large masses and small differences between the masses.

Ar is not frozen at the 50-K deposition temperature. Decreasing the deposition temperature to 27 or 22 K results in an amount of *frozen* Ar that decreases as the deposition rate decreases (Fig. 2a), as described above. The decrease at 27 K is steeper than that at 22 K. Yet, the amount of *internally trapped* Ar (deposition at 27 or 22 K) does not decrease when the deposition rate decreases from 10^{-1} to $10^{-4} \mu\text{m min}^{-1}$. However, at $10^{-5} \mu\text{m min}^{-1}$ the amount does decrease.

At such low deposition rates we must consider also the background in the chamber, which is mainly background air N_2 plus CO emitted from the stainless steel walls, both having $m/e = 28$. The N_2 and CO molecules compete with Ar to enter the open ice pores. The competition is more significant when the deposition rate is so slow that the Ar flux, flowed with the water-vapor and the “background” Ar, are lower than the $\text{N}_2 + \text{CO}$ background. Introducing an Ar + water-vapor mixture at the very low rate of $10^{-5} \mu\text{m min}^{-1}$ into the chamber at room temperature, we found that the Ar abundance is about two orders of magnitude lower

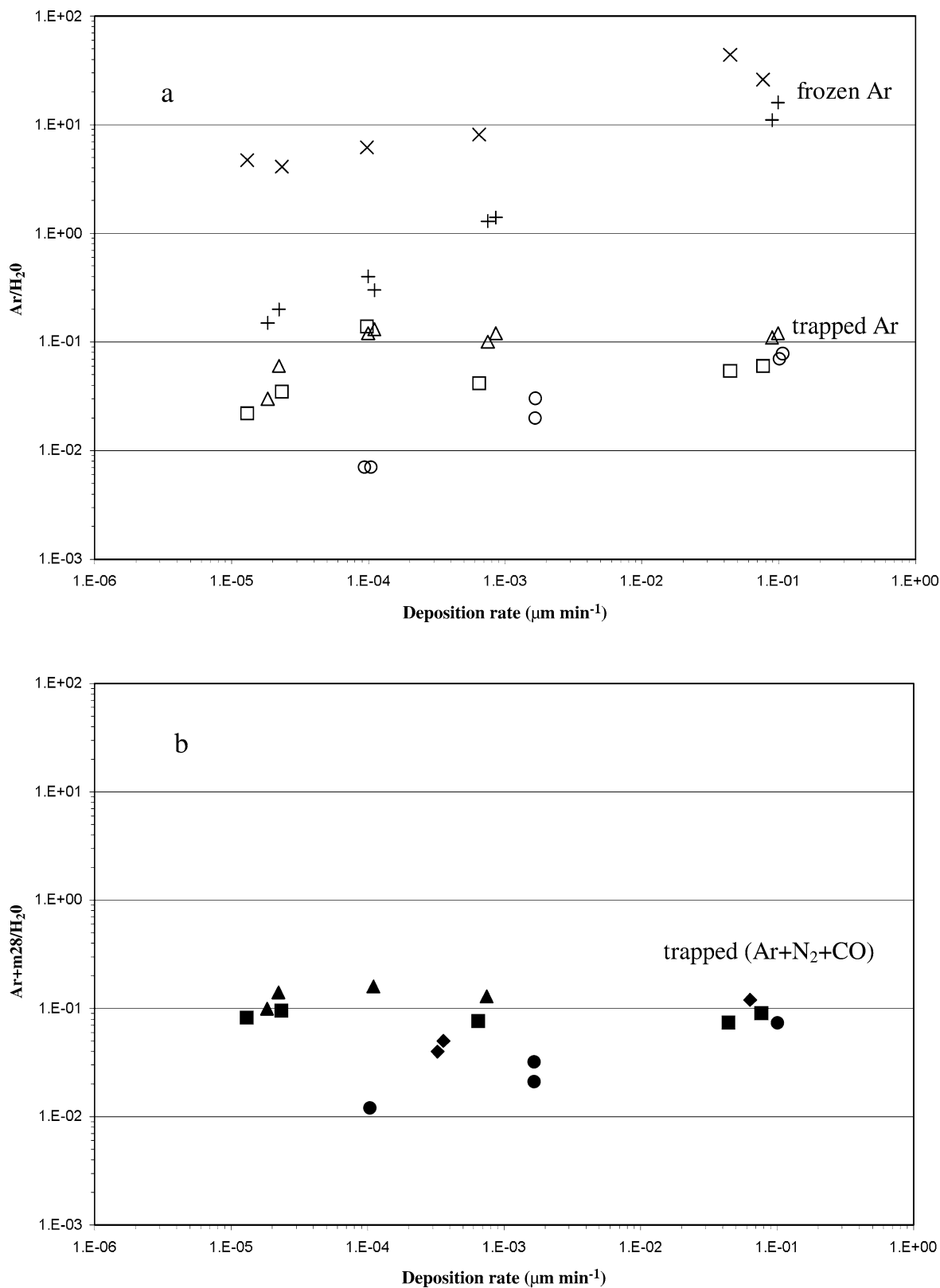


Fig. 2. The ratios of gases/H₂O in water ice formed from H₂O:Ar = 1:1 mixtures, at three different temperatures, as a function of deposition rate. (a) The amount of frozen Ar that evaporates, or trapped Ar that is released from the ice: frozen Ar from deposition at 27 K (+) and 22 K (×). Trapped Ar from deposition at 50 K (○), 27 K (△), and 22 K (□). (b) The amount of Ar + N₂ + CO trapped in water ice formed at 50 K (●), 37 K (◆), 27 K (▲), and 22 K (■) from the same experiments shown in (a). Note that at 50 and 37 K (●, ◆) the amount of trapped gases decreases with the decrease in the deposition rate, while at 27 and 22 K (▲, ■) it remains constant. Note also the small scatter of the experimental results between duplicate runs.

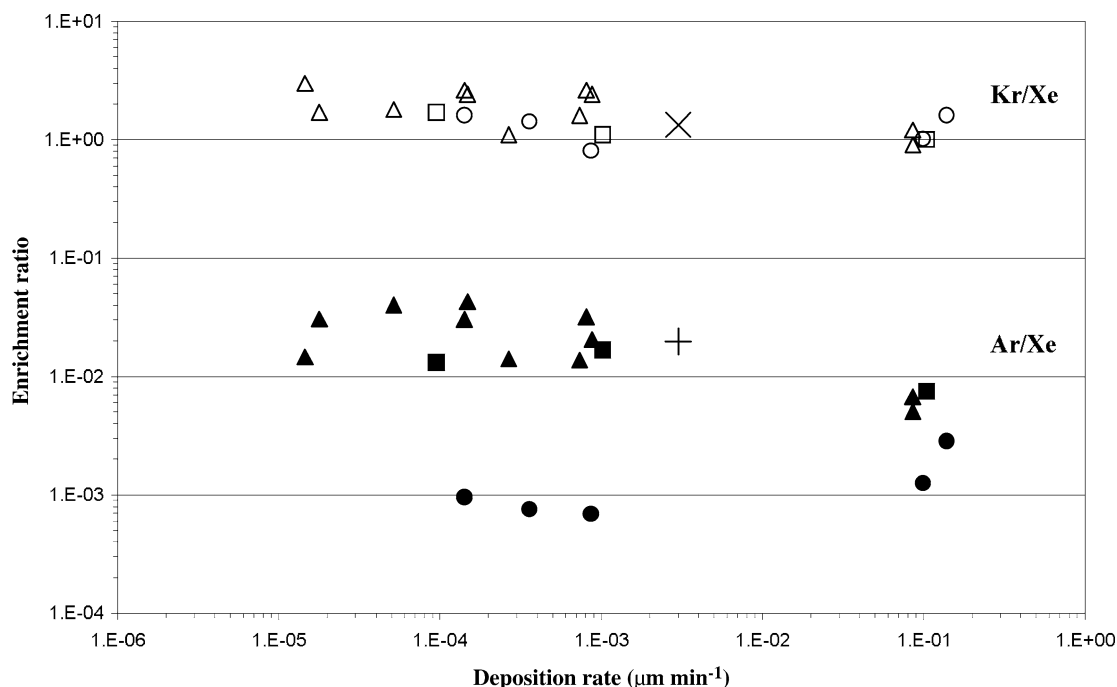


Fig. 3. Enrichment ratios (the ratio Kr/Xe or Ar/Xe trapped in the ice, divided by the ratio Kr/Xe or Ar/Xe in the gas mixture deposited together with water vapor on the cold plate) as a function of deposition rate: Kr/Xe in water ice deposited at 50 K (○), 27 K (△), and 22 K (□); Ar/Xe in water ice deposited at 50 K (●), 27 K (▲), and 22 K (■). We marked also the enrichment ratios in Earth's atmosphere, Kr/Xe (×) and Ar/Xe (+), which fit well the experimental values.

than that of the N_2+CO background. However, during the deposition process the Ar:water-vapor mixture is flowed directly onto the plate, while the N_2+CO background is ambient and is only about one order of magnitude lower in a cold chamber than in the room temperature chamber. This is due to the freezing of part of the background gases on the cold finger. It should be noted that the ratio $H_2O:CO$ observed in the Orion dark cloud ranges from 0.1 to 1 in the gas phase (Van Dishoeck et al., 1993). This range suits our $H_2O:Ar:(N_2+CO) = 1:1:(\sim 10)$ mixture. We measured the $m/e = 28$ flux, in addition to the Ar and water-vapor fluxes, during the warming up of the ice and calculated the total amount of gases trapped in the ice. The results are shown in Fig. 2b. Comparing this figure with 2a we see that the amount of trapped N_2+CO , relative to the amount of trapped Ar, increases as the deposition rate decreases. However, most importantly, the total amount of trapped gas (Ar + N_2 + CO) remains constant, about 10% relative to water, at all deposition rates, except at $T = 50$ K. Evidently the reason for the decrease in trapped Ar at the $10^{-5} \mu m \min^{-1}$ deposition rate (Fig. 2a) is the successful competition for pore spaces by the background gases in the chamber at this very slow rate. We conclude that in the absence of such competition, the amount of trapped Ar would not decrease and our assumption that the atoms of Ar have insufficient energy to escape from the pores at these low temperatures is valid. However, at 50 K and even at 37 K, the amount of trapped gas decreases with the decrease in the deposition rate and is below 10% at the lowest rates.

Enrichment ratios

Once we established that it is possible to trap $\sim 10\%$ CO (Ar) in water ice at 27–22 K, we wanted to study the Ar/Kr/Xe enrichment factors at these low temperatures and low deposition rates, in order to find out whether these enrichment factors can account for Earth's and Mars' noble gas ratios.

The enrichment ratios of the heavy noble gases Ar, Kr, and Xe when trapped in water ice formed at 50, 27, and 22 K are shown in Fig. 3. It should be noted that Ar, Kr, and Xe do not freeze on the ~ 90 -K radiation shield, nor are they trapped in the ~ 90 -K water ice on it. Thus their ratios in the chamber and in the gas emanating from the ice are not altered. The enrichment ratio (the ratio between the gases in the ice, divided by their ratio in the gas mixture) for Kr/Xe does not change with the deposition temperature (50, 27, or 22 K) or by decreasing the deposition rate by four orders of magnitude. The enrichment ratio Ar/Xe is higher at deposition temperatures of 27 and 22 K than at 50 K, and most important, it does not change with the deposition rate at low rates. We cannot explain the small decrease at 22 and 27 K for the highest deposition rate. Obviously, the heavier and more polarizable Kr and Xe are trapped in the ice more efficiently than Ar. The enrichment ratios Kr/Xe and Ar/Xe, at 22–27 K, are 2.0 ± 0.6 and 0.025 ± 0.01 , respectively. We considered only the amount of trapped gases, since the amount of frozen Ar is very small at very low deposition rates and the small amounts of Kr and Xe in the gas mixture

are not frozen but trapped in the ice. In the region in space where the real ice grains formed, the gas mixture was Ar:Kr:Xe = 69000:21:1 with H₂O and CO being two orders of magnitude higher. In the experiments, Ar, Kr, and Xe were trapped in water ice in the presence of ~10 times more N₂+CO as a background gas in the experimental chamber.

Implications for comets

The ice grains that formed the comets were formed themselves at a very slow rate, perhaps 0.1 μm/millions of years. Because the amount of trapped gas in our experiments at 22 and 27 K remains unchanged at about 10% relative to water (Figs. 2a, 2b), we may extrapolate our results to this very low deposition rate. We can conclude that the grains' formation temperature was 22–27 K. Had the temperature been ~10 K, we expect a large fraction of frozen Ar (CO) in addition to the trapped Ar (CO), much more than the observed ~10% and no fractionation among the frozen gases (Bar-Nun and Kleinfeld, 1989). The amount of frozen gas decreases to about 10⁻⁵ relative to water (extrapolating to 10⁶ years) at a deposition temperature of 27 K and to 0.04 at 22 K. Most of the gas in cometary ice is therefore trapped in the water ice and only, if at all, a small amount freezes. Even less volatile gases, such as CO₂, which is found in comets, at ~3% relative to water, do not freeze under these conditions. Addition of 1% CO₂ to a water vapor:Ar = 1:1 mixture, at 25 K and at the highest deposition rate (10⁻¹ μm min⁻¹), results in 0.04 CO₂ (relative to water) trapped in the ice and only 0.006 as frozen CO₂ (Notesco and Bar-Nun, in preparation).

The ice formation temperature of 22–27 K is in agreement with the nuclear spin temperature of ~25 K, derived from the ortho/para ratio of H₂O in Comet Halley (Mumma et al., 1988) and Comet Hale-Bopp (Crovisier, 1999), and the ortho/para ratio of NH₃ in Comet LINEAR C/1999S4 ~28 K (Kawakita et al., 2001). This may simply be a coincidence, but it may also signify that the temperature at which the ice grains formed was in fact the temperature at which the nuclear spins of the constituent hydrogen atoms were set to their currently observed values. If this were true, it would point toward the ISM as the place where the ice grains formed.

The relatively small amount of CO (~1%) observed in Comet LINEAR 1999/S4 (Bockelée-Morvan et al., 2001; Mumma et al., 2001) may be a result of formation at a somewhat higher temperature (> 27 K) as these authors have suggested, because at a temperature of 50 K the amount of trapped gas decreases and becomes ~1% already at a deposition rate of 10⁻⁴ μm min⁻¹, decreasing further at lower deposition rates (Fig. 2).

The enrichment ratios of the most abundant nonradiogenic heavy noble gases in Earth's atmosphere (atmospheric ratios divided by the solar ratios) are ⁸⁴Kr/¹³²Xe = 1.4 and ³⁶Ar/¹³²Xe = 0.02. These values fit well the enrichment ratios of these gases when trapped in cometary water ice

(Fig. 3). This is perhaps the most important result from this work: even at low temperatures, the same fractionation of the noble gases that we observe in the atmospheres of Earth and Mars is established by trapping in amorphous ice, if the flow rates have the low values that we expect are more realistic of the natural setting. This similarity in noble gas fractionation suggests a cometary contribution to the atmosphere, as we have proposed earlier (Owen et al., 1991, 1992; Owen and Bar-Nun, 1993).

Acknowledgments

This research was supported by Grant 2000005 from the U.S.–Israel Binational Science Foundation (BSF), Jerusalem, Israel and in part by NASA, under Grant NAGW 2631. We thank the two anonymous reviewers for very helpful suggestions.

References

- Bar-Nun, A., Kleinfeld, I., 1989. On the temperature and gas composition in the region of comet formation. *Icarus* 80, 243–253.
- Bar-Nun, A., Herman, G., Laufer, D., Rappaport, M.L., 1985. Trapping and release of gases by water ice and implications for icy bodies. *Icarus* 63, 317–332.
- Bar-Nun, A., Dror, J., Kochavi, E., Laufer, D., 1987. Amorphous water ice and its ability to trap gases. *Phys. Rev. B* 35, 2427–2435.
- Bar-Nun, A., Kleinfeld, I., Kochavi, E., 1988. Trapping of gas mixtures by amorphous water ice. *Phys. Rev. B* 38, 7749–7754.
- Bockelée-Morvan, D., and 18 colleagues, 2001. Outgassing behavior and composition of comet C/1999 S4 (LINEAR) during its disruption. *Science* 292, 1339–1343.
- Crovisier, J., 1999. Infrared observations of volatile molecules in Comet Hale-Bopp. *Earth Moon Planets* 79, 125–143.
- Delsemme, A.H., 1991. Nature and history of the organic compounds in comets: an astrophysical view, in: Newburn Jr., R.L., Neugebauer, M., Rahe, J. (Eds.), *Comets in the Post Halley Era*, Kluwer, Dordrecht, pp. 417–428.
- Delsemme, A.H., 2000. 1999 Kuiper Prize Lecture: cometary origin of the biosphere. *Icarus* 146, 313–325.
- Jenniskens, P., Blake, D.F., 1994. Structural transitions in amorphous water ice and astrophysical implications. *Science* 265, 753–756.
- Jenniskens, P., Blake, D.F., 1996. Crystallization of amorphous water ice in the solar system. *Astrophys. J.* 473, 1104–1113.
- Kawakita, H., and 18 colleagues, 2001. The spin temperature of NH₃ in Comet C/1999S4 (LINEAR). *Science* 294, 1089–1091.
- Laufer, D., Kochavi, E., Bar-Nun, A., 1987. Structure and dynamics of amorphous water ice. *Phys. Rev. B* 36, 9219–9227.
- Laufer, D., Notesco, G., Bar-Nun, A., 1999. From the interstellar medium to Earth's oceans via comets—an isotopic study of HDO/H₂O. *Icarus* 140, 446–450.
- Mumma, M.J., Blass, W.E., Weaver, H.A., Larson, H.P., 1988. Measurements of the ortho-para ratio and nuclear spin temperature of water vapor in Comets Halley and Wilson (19861) and implications for their origin and evolution. *Bull. Am. Astron. Soc.* 20, 826.
- Mumma, M.J., Dello Russo, N., DiSanti, M.A., Magee-Sauer, K., Novak, R.E., Brittain, S., Rettig, T., McLean, I.S., Reuter, D.C., Xu, Li-H., 2001. Organic composition of C/1999 S4 (LINEAR): a comet formed near Jupiter? *Science* 292, 1334–1339.

- Notesco, G., Bar-Nun, A., 1997. Trapping of methanol, hydrogen cyanide, and n-hexane in water ice, above its transformation temperature to the crystalline form. *Icarus* 126, 336–341.
- Notesco, G., Kleinfeld, I., Laufer, D., Bar-Nun, A., 1991. Gas release from comets. *Icarus* 89, 411–413.
- Notesco, G., Laufer, D., Bar-Nun, A., 1997. The source of high CH_6/CH_4 ratio in Comet Hyakutake. *Icarus* 125, 471–473.
- Notesco, G., Laufer, D., Bar-Nun, A., 1999a. An experimental study of the isotopic enrichment in Ar, Kr, and Xe when trapped in water ice. *Icarus* 142, 298–300.
- Notesco, G., Laufer, D., Bar-Nun, A., 1999b. The formation temperature of Comets Halley, Hyakutake and Hale-Bopp. *Earth Moon Planets* 77, 237.
- Owen, T., Bar-Nun, A., 1993. Noble gases in atmospheres. *Nature* 361, 693–694.
- Owen, T., Bar-Nun, A., 1995. Comets impacts and atmospheres. *Icarus* 116, 215–226.
- Owen, T., Bar-Nun, A., 2000. Volatile contribution from icy planetesimals, in: Canup, R., Righter, K. (Eds.), *Origin of the Earth and Moon*, Univ. of Arizona Press, Tucson, pp. 459–471.
- Owen, T., Bar-Nun, A., Kleinfeld, I., 1991. Noble gases in terrestrial planets: evidence for cometary impacts?, in: Newburn Jr., R.L., Neugebauer, M., Rahe, J. (Eds.), *Comets in the Post-Halley Era I*, Kluwer Academic, the Netherlands, pp. 429–437.
- Owen, T., Bar-Nun, A., Kleinfeld, I., 1992. Possible cometary origin of heavy noble gases in the atmospheres of Venus, Earth and Mars. *Nature* 358, 43–46.
- Sill, G.T., Wilkening, L., 1978. Ice clathrate as a possible source of the atmospheres of the terrestrial planets. *Icarus* 33, 13–27.
- Van Dishoeck, E.F., Blake, G.A., Draine, B.T., Lunine, J.I., 1993. The chemical evolution of protostellar and protoplanetary matter, in: Levy, E.H., Lunine, J.I. (Eds.), *Protostars and Planets III*, Univ. of Arizona Press, Tucson, pp. 163–241.